European Congress on Computational Methods
in Applied Sciences and Engineering (ECCOMAS 2012)
J. Eberhardsteiner et.al. (eds.)
Vienna, Austria, September 10-14, 2012

A WEAKLY COMPRESSIBLE FORMULATION FOR MODELLING LIQUID-GAS SLOSHING

Johan A. Heyns[1], **Oliver F. Oxtoby**[1], **and Arnaud G. Malan**[2]

[1]Aerospace Systems Competency, Council for Scientific and Industrial Research
P.O. Box 395, Pretoria 0001, South Africa
e-mail: jheyns@csir.co.za, ooxtoby@csir.co.za

[2] Mechanical Engineering, University of Cape Town
Private Bag X3, Rondebosch, 7701, South Africa

Keywords: Free-surface modelling, weakly compressible, GMRES

Abstract. *This study presents the development and extension of free-surface modelling techniques with the purpose of improving the modelling accuracy for liquid-gas sloshing. Considering high density ratio fluids under low Mach number conditions, the implementation of a weakly compressible formulation which accounts for variations in the gas density is presented. With the aim of ensuring a computational efficient implementation of the proposed formulation, an implicit iterative GMRES solver with LU-SGS preconditioning is employed. To evaluate the weakly compressible formulation a partially filled tank subjected to lateral excitation is numerically modelled. Pressures predicted by the weakly compressible formulation are compared to that of an incompressible solver as well as results obtained experimentally. For the problem considered, it is demonstrated that the weakly compressible formulation provides an accurate approximation of the experimental results and offers a notable improvement over the incompressible solver.*

1 INTRODUCTION

Various industries benefit from the accurate modelling of multi-fluid liquid-gas flow. Examples include maritime and naval engineering which require the accurate prediction of wave impact loads on fixed and floating structures. Furthermore, with the transportation of liquids it is necessary to accurately describe the two-fluid flow as it greatly influences sloshing induced impact pressures measured on container walls. In commercial aircraft, for example, fuel can constitute a significant portion of take off weight and may be subjected to highly dynamic loading conditions. On liquefied natural gas (LNG) carriers stringent restrictions are placed on tank filling levels due to potentially large sloshing induced loads. With the aim of modelling immiscible liquid-gas flow accurately and efficiently, Computational Fluid Dynamics (CFD) is increasingly employed as it has in recent years developed to a point where it can provide a cost effective alternative.

Most existing liquid-gas free-surface models treat both gas and liquid as incompressible [21, 11, 12, 19], neglecting the effect of density changes due to pressure variations. Although this is a reasonable assumption for most free-surface flow regimes, in high density ratio systems entrapped gas pockets may be subjected to notable fluctuations in pressure. In these cases the compressibility of the gas cannot be neglected as it would influence the predicted pressures [10, 6, 13, 2]. To account for these variations in gas density, a weakly compressible formulation for liquid-gas flow is presented and implemented in the *Elemental* software [15, 16].

For industrial sized problems it is found that a significant number of discrete volumes are required to ensure an accurate approximation. Analysing unsteady free-surface flow, therefore, involves the solution of numerous time steps, resulting in simple matrix-free solvers such as Jacobi time-stepping being prohibitively inefficient. To circumvent this a Generalised Minimum Residual (GMRES) solver with Lower-Upper Symmetric Gauss-Seidel (LU-SGS) preconditioning is employed.

To evaluate the weakly compressible liquid-gas solver, which accounts for variations in gas density, a partially filled tank subjected to lateral excitation is considered. The results form the weakly compressible formulation are compared to the numerical results from an incompressible formulation as well as experimental measurements [1].

2 WEAKLY COMPRESSIBLE LIQUID-GAS FLOW

Using the Eulerian volume-of-fluid (VOF) approach a control volume partially filled with liquid and gas can be considered, where the volume fraction occupied by the liquid and the gas are respectively denoted α and $1-\alpha$. For a given cell an averaged velocity, $u_l = u_g = u$, and pressure, $p_l = p_g = p$, can be assumed if a homogeneous flow model is employed. Dias et al. [5] note that this is an accurate approximation if the time scales on which the turbulent drag forces tend to equalise the velocity are much smaller than the time scales on which the flow is averaged. The resulting averaged liquid-gas momentum equation reads

$$\frac{\partial(\rho u_i)}{\partial t} + \frac{\partial(\rho u_i u_j)}{\partial x_j} + \frac{\partial p}{\partial x_i} = S_i \tag{1}$$

The source term, $\mathbf{S}$, contain the hydro-static pressure term as well as viscous term and if Newtonian flow is assumed, the following holds

$$S_i = \rho g_i + \frac{\partial}{\partial x_j}\left(\mu \frac{\partial u_i}{\partial x_j}\right) \tag{2}$$

where the gravitational acceleration is denoted g and $\mathbf{x}$ is the Cartesian spatial coordinate. In the previous equation time is denoted t and the mixture density and dynamic viscosity can be calculated from the volume fractions

$$\begin{aligned}\rho &= \alpha\rho_l + (1-\alpha)\rho_g \\ \mu &= \alpha\mu_l + (1-\alpha)\mu_g\end{aligned}$$

where the density and viscosity are denoted ρ and μ. The subscripts l and g are used to represented the liquid and gas.

The evolution of the liquid-gas interface is approximated using an advective volume fraction equation

$$\frac{\partial\alpha}{\partial t} + \frac{\partial(\alpha u_j)}{\partial x_j} = 0 \tag{3}$$

Considering weakly compressible low Mach number flow conditions, the continuity equation which accounts for barotropic variations in gas density reads [7]

$$\frac{(1-\alpha)}{\rho_g}\frac{\partial\rho_g}{\partial t} = -\frac{\partial u_j}{\partial x_j} \tag{4}$$

where the conditional temporal term is only activated in the gas phase.

As it is assumed that the gradient in the gas density is negligible small, it is required that the hydro-static source term in the gas phase also be neglected to ensure consistency in the momentum equation. This is, however, acceptable as the hydro-static pressure is a function of the density and is typically three orders of magnitude smaller for the gas than the liquid.

Finally, the compression and expansion of the gas is approximated using a linear form of the ideal gas law

$$\rho_g - \rho_g^o = \frac{1}{c_g^2}(p - p^o) \tag{5}$$

where ρ^o and p^o are the initial density and pressure.

3 NUMERICAL MODEL

3.1 Spatial discretisation

The governing equations are discretised using an unstructured vertex-centred edge-based finite volume approach. This approach is preferred as it found to be is computationally [14] as well as memory efficient [4, 22]. Further, the edge-based matrix-free implementation ensures an efficient extension to parallel computing.

The governing equations can be represented a single unified equation

$$\mathbf{A}\frac{\partial\mathbf{W}}{\partial t} + \frac{\partial\mathbf{F}^j}{\partial x_j} - \frac{\partial\mathbf{G}^j}{\partial x_j} = \mathbf{S} \tag{6}$$

where

$$\begin{aligned}\mathbf{W} &= \begin{pmatrix}\alpha\\ \rho_g\\ \rho u_i\end{pmatrix},\ \mathbf{F}^j = \begin{pmatrix}\alpha u_j\\ u_j\\ \rho u_i u_j + \delta_{ij}p\end{pmatrix},\ \mathbf{G}^j = \begin{pmatrix}0\\ 0\\ \mu\frac{\partial u_i}{\partial x_j}\end{pmatrix}, \\ \mathbf{A} &= \begin{pmatrix}1 & 0 & 0\\ 0 & \frac{1-\alpha}{\rho_g} & 0\\ 0 & 0 & 1\end{pmatrix},\ \mathbf{S} = \begin{pmatrix}0\\ 0\\ \alpha\rho_l g_i\end{pmatrix}\end{aligned}$$

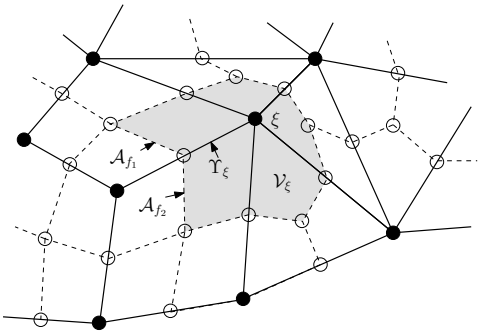

Figure 1: Schematic construction of the median-dual-mesh on hybrid grids

With the said finite volume approach, the spatial domain, $\mathcal{V}$, is subdivided into a finite number of non-overlapping volumes, $\mathcal{V}_\xi \in \mathcal{V}$. The dual-mesh construction for the vertex-centred approach as proposed by Vahdati et al. [20] is illustrated in Figure 1. The general governing equation can be cast into weak form by integrating over the finite volume, $\mathcal{V}_\xi$, and be written in terms of surface integrals

$$\int_{\mathcal{V}_\xi} \mathbf{A}\frac{\partial \mathbf{W}}{\partial t} d\mathcal{V} + \int_{\mathcal{A}_\xi} (\mathbf{F}^j - \mathbf{G}^j) n_j d\mathcal{A} = \int_{\mathcal{V}_\xi} \mathbf{S} d\mathcal{V} \tag{7}$$

where $\mathcal{A}_\xi$ is the surface bounding $\mathcal{V}_\xi$ and $\mathbf{n}$ is the unit vector normal to the boundary segment $\mathcal{A}$ pointing outward. The bounding surface information stored in edge-coefficients are defined as $\mathbf{C}_f = \mathbf{n}_{f_1}\mathcal{A}_{f_1} + \mathbf{n}_{f_2}\mathcal{A}_{f_2}$.

3.2 Upwind split solver

The continuity and momentum equations are solved using an upwind-stabilised pressure-projection explicit split [18] with artificial compressibility. It consists of a three step procedure, first an intermediate momentum equation, from which the pressure gradients are removed, is solved explicitly viz.

$$\frac{\Delta \rho u_i^*}{\Delta t} = -\frac{\partial (\rho u_i u_j)}{\partial x_j}\bigg|^n + \frac{\partial}{\partial x_j}\left(\mu \frac{\partial u_i}{\partial x_j}\right)^n \tag{8}$$

where $\Delta \rho u_i^* = \rho u_i^* - \rho u_i|^n$ and $\Delta t = t^{n+1} - t^n$.

Next, the pressure is calculated via an implicit pressure–projection equation with artificial compressibility

$$\begin{aligned} \frac{1}{c_\tau^2}\frac{p^{\tau+1} - p^\tau}{\Delta t_\tau} &= -\frac{\partial}{\partial x_j}\left[u_j^\tau + \Delta u_j^* + \frac{\Delta t}{\rho}\left(-\frac{\partial p^{\tau+1}}{\partial x_j} + \alpha \rho_l g\right)\right] \\ &\quad -\frac{(1-\alpha)}{\rho_g}\frac{1}{c_g^2}\frac{p^{\tau+1} - p^n}{\Delta t} \end{aligned} \tag{9}$$

where $p^{\tau+1}$ is the pressure being solved for in a specific iteration and Δt_τ the pseudo time step size. The artificial acoustic velocity c_τ is calculated as proposed by Malan et al. [15].

Finally, the velocities are calculated from the corrected momentum equation which contain the updated values

$$\frac{\rho u_i^{n+1} - \rho u_i^n}{\Delta t} = \frac{\Delta \rho u_i^*}{\Delta t} - \frac{\partial p^{n+1}}{\partial x_i} + \alpha \rho_l g \tag{10}$$

3.3 Volume-of-fluid equation

The volume-of-fluid equation (3) remains unchanged from the incompressible free-surface flow and existing VOF surface capturing schemes [3, 19, 17, 9] may be employed. For this study a blended higher-resolution artificial compressive scheme (HiRAC), as proposed by [8], is used. The VOF equation is discretised using second order Crank-Nicholson so that the semi-discrete form of the VOF equation reads

$$\frac{\alpha^{n+1}-\alpha^n}{\Delta t} = -\frac{1}{2}\left[\frac{\partial(u_i\alpha)}{\partial x_i}\bigg|^{n+1} + \frac{\partial(u_i\alpha)}{\partial x_i}\bigg|^{n}\right] - \frac{\partial}{\partial x_i}[u_c|_i\alpha(1-\alpha)] \tag{11}$$

where the artificial term, which is only activated in the interface, reduces the smearing of the free-surface interface through the compressive velocity, u_c. The volume fraction face value, α_f, is interpolated using a blended high-resolution scheme, which switches between a compressive and more diffusive scheme based on the alignment of the interface with the mesh.

4 RESULTS

A partially filled tank with baffle configuration under lateral excitation is modelled using both a weakly compressible solver, accounting for variations in density, as well as an incompressible solver. The numerical results are compared to pressures obtained from experimental measurements [1]. A schematic of the tank is shown in Figure 2a. The tank is 75 % filled with liquid and is subjected to sinusoidal lateral excitation where the maximum amplitude of displacement is 0.113 m and the excitation frequency is 1.5 Hz. It is found that for these conditions significant mixing of the liquid and gas occurs.

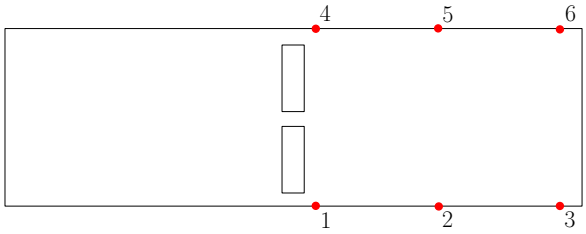

(a) Schematic representation

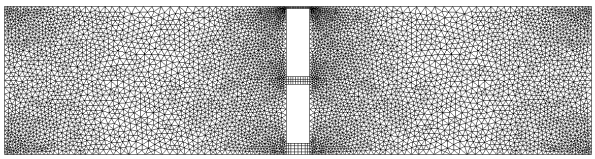

(b) Hybrid unstructured mesh

Figure 2: Partially filled tank with baffle subjected to lateral excitation

For the analysis a hybrid unstructured mesh with 6000 nodes shown in Figure 2b is employed and viscous boundary conditions are specified on the tank walls. Furthermore, the material properties as given in Table 1 and a gravitational acceleration of $g = 9.81$ m/s^2 is used.

In Figures 3a to 3d the numerical and experimental results are compared for the various points indicated on Figure 2a. As only relative pressures can be calculated for the incompressible flow, the pressures relative to a chosen point of reference are plotted. For the purpose of this study point 5, which is situated at the top middle of the right-hand chamber, is used as reference.

Table 1: Material properties of the liquid and gas

	Liquid (Water)	Gas (Air)
Density ($\mathrm{kg/m^3}$)	998	1.21
Viscosity ($\mathrm{kg/m\,s}$)	1.002×10^{-3}	1.812×10^{-6}
Acoustic velc ($\mathrm{m/s}$)	–	343.2

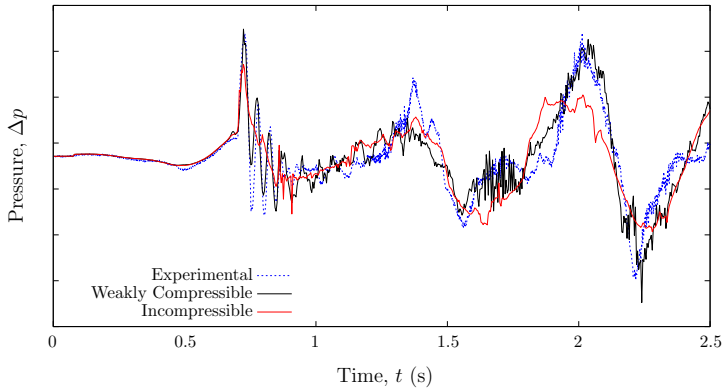

(a) Point 1, bottom left

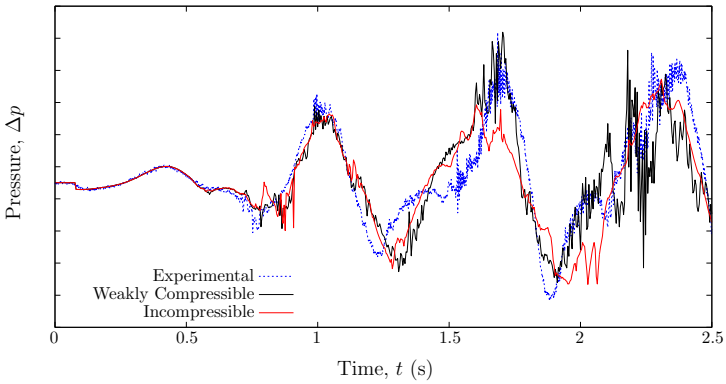

(b) Point 3, bottom right

Figure 3: Comparison of measured and predicted relative pressures

From these figures it appears the weakly compressible formulation, when compared to the incompressible formulation, provides a better representation of the experimentally measured pressures. This is in particularly evident just after the liquid hits the top opening at $t = 0.75$ s and prevents the movement of gas between the two chambers. During this time, the gas is entrapped and the weakly compressible formulation captures the oscillatory behaviour noted in the experimental results. It is also found that at a number of measuring points the weakly compressible formulation predicts the maximum and minimum pressures more accurately. Examples of these are at $t = 1$ s at point 6; $t = 1.7$ s at points 3 and 6; $t = 2.0$ s at points 1 and 4; as well as $t = 2.25$ s at points 1 and 4.

It is found that the additional computational overhead for the weakly compressible formulation when compared with the incompressible formulation is negligible. Furthermore, it is found that for the problem considered, the new weakly compressible formulation greatly improves the rate of convergence, reducing the computational time by approximately 30 %. By accounting for variations in gas density, it is suspected, the numerical system is softened and results in the

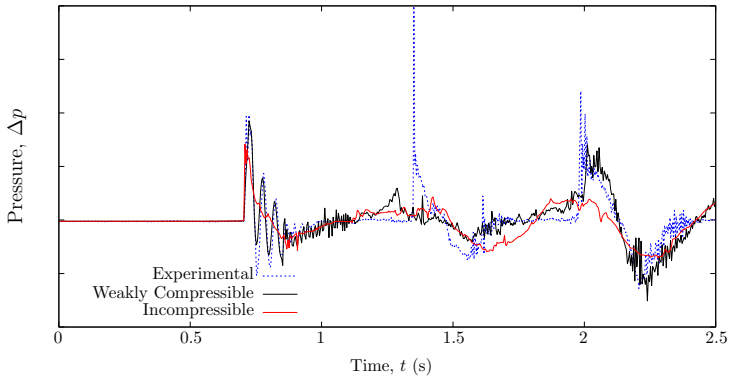

(c) Point 4, top left

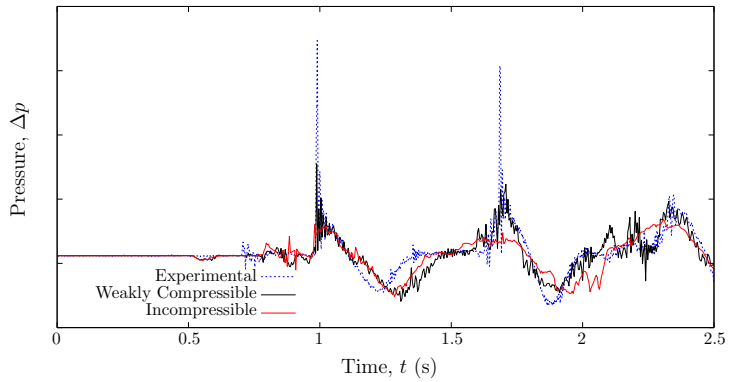

(d) Point 6, top right

Figure 3: Comparison of measured and predicted relative pressures

improved convergence rates.

5 CONCLUSIONS

This work presents a weakly-compressible formulation for liquid-gas flow, which accounts for variations in gas density. The formulation is evaluated by modelling a partially filled tank with baffle configuration under lateral excitation. The numerical predicted pressures are compared to that of an incompressible formulation as well as experimental measured results. Although the incompressible formulation provides an accurate representation of the experimental results, it is found that by accounting for variations in gas density the weakly compressible formulation offers a notable improvement in predicting liquid-gas sloshing induced loads. Furthermore, it is found that with liquid-gas sloshing as considered in this study, the weakly compressible formulation provides improved convergence rates and, therefore, reduces the computational time.

REFERENCES

[1] BEELAB test reference BAE808: Laboratory simulation of sloshing in part-filled tanks, 2008.

[2] GN Bullock, C. Obhrai, DH Peregrine, and H. Bredmose. Violent breaking wave impacts. Part 1: Results from large-scale regular wave tests on vertical and sloping walls. *Coastal Engineering*, 54(8):602–617, 2007.

[3] M. Darwish and F. Moukalled. Convective schemes for capturing interfaces of free-surface flows on unstructured grids. *Numerical Heat Transfer, Part B: Fundamentals*, 49(1):19–42, 2006.

[4] B. de Foy and W. Dawes. Unstructured pressure-correction solver based on a consistent discretization of the Poisson equation. *International Journal for Numerical Methods in Fluids*, 34:463–478, 2000.

[5] F. Dias, D. Dutykh, and J.M. Ghidaglia. A two-fluid model for violent aerated flows. *Computers & Fluids*, 39(2):283–293, 2010.

[6] OM Faltinsen, OF Rognebakke, and AN Timokha. Classification of three-dimensional nonlinear sloshing in a square-base tank with finite depth. *Journal of Fluids and Structures*, 20:81–103, 2005.

[7] J. A. Heyns, T. M. Harms, and A. G. Malan. Free-surface modelling technology for compressible and violent flows. In *41st AIAA Fluid Dynamics Conference and Exhibit, Honolulu, Hawaii, 27-30 June*, 2011.

[8] J. A. Heyns, A. G. Malan, T. M. Harms, and O. F. Oxtoby. Development of a compressive surface capturing formulation for modelling free-surface flow using the volume-of-fluid approach. *International Journal for Numerical Methods in Fluids*, 2012.

[9] B. Lafaurie, C. Nardone, R. Scardovelli, S. Zaleski, and G. Zanetti. Modelling merging and fragmentation in multiphase flows with SURFER. *Journal of Computational Physics*, 113(1):134–147, 1994.

[10] DH Lee, MH Kim, SH Kwon, JW Kim, and YB Lee. A parametric sensitivity study on LNG tank sloshing loads by numerical simulations. *Ocean Engineering*, 34(1):3–9, 2007.

[11] D. Liu and P. Lin. Three-dimensional liquid sloshing in a tank with baffles. *Ocean Engineering*, 36:202–212, 2009.

[12] R. Löhner, C. Yang, and E. Oñate. On the simulation of flows with violent free surface motion. *Computer Methods in Applied Mechanics Engineering*, 195:5597–5620, 2006.

[13] C. Lugni, M. Brocchini, and OM Faltinsen. Wave impact loads: The role of the flip-through. *Physics of fluids*, 18, 2006.

[14] H. Luo, J. D. Baum, and R. Löhner. Edge-based finite-element scheme for the Euler equations. *AIAA*, 32(6):1183–1190, 1994.

[15] A. G. Malan, R. W. Lewis, and P. Nithiarasu. An improved unsteady, unstructured, artificial compressibility, finite volume scheme for viscous incompressible flows: Part I. Theory and implementation. *International Journal for Numerical Methods in Engineering*, 54(5):695–714, 2002.

[16] A. G. Malan, R. W. Lewis, and P. Nithiarasu. An improved unsteady, unstructured, artificial compressibility, finite volume scheme for viscous incompressible flows: Part II. Application. *International Journal for Numerical Methods in Engineering*, 54(5):715–729, 2002.

[17] S. Muzaferija, M. Peric, P. Sames, and T. Schellin. A two-fluid Navier-Stokes solver to simulate water entry. In *Proc 22nd Symposium on Naval Hydrodynamics*, pages 277–289, 1998.

[18] O. F. Oxtoby and A. G. Malan. A matrix-free, implicit, incompressible fractional-step algorithm for fluid-structure interaction applications. *J. Comput. Phys.*, 2012.

[19] O. Ubbink and R. I. Issa. A method for capturing sharp fluid interfaces on arbitrary meshes. *Journal of Computational Physics*, 153:26–50, 1999.

[20] M. Vahdati, K. Morgan, J. Peraire, and O. Hassan. A cell-vertex upwind unstructured grid solution procedure for high-speed compressible viscous flow. In *Proceedings at the International Conference on Hypersonic Aerodynamics*, pages 12.1–12.22, London, 1989. Royal Aeronautical Society.

[21] T. Wacławczyk and T. Koronowiczy. Modeling of the wave breaking with CICSAM and HRIC high-resolution schemes. In S. Wesseling, E. Oñate, and J. Périaux, editors, *European Conference on Computational Fluid Dynamics ECCOMAS CFD*, 2006.

[22] Y. Zhao and B. Zhang. A high-order characteristics upwind FV method for incompressible flow and heat transfer simulation on unstructured grids. *International Journal of Numerical Methods in Engineering*, 37:3323–3341, 2000.